Annals of Glaciology 35 2002

Electrical measurements on the 2503 m Dome F Antarctic ice core

Shuji FUJITA,[1,3] Nobuhiko AZUMA,[2] Hideaki MOTOYAMA,[3] Takao KAMEDA,[4] Hideki NARITA,[5] Yoshiyuki FUJII,[3] Okitsugu WATANABE[3]

[1]*Department of Applied Physics, Graduate School of Engineering, Hokkaido University, Sapporo 060-8628, Japan*
E-mail: sfujita@pmg.nipr.ac.jp

[2]*Department of Mechanical Engineering, Nagaoka University of Technology, 1603-1 Kamitomioka, Nagaoka 940-2188, Japan*

[3]*National Institute of Polar Research, Kaga, Itabashi-ku, Tokyo 173-8515, Japan*

[4]*Kitami Institute of Technology, 165, Koencho, Kitami 090-8507, Japan*

[5]*Institute of Low Temperature Science, Hokkaido University, Sapporo 060-0819, Japan*

ABSTRACT. The 320 kyr climatic record from the 2503 m Dome Fuji (Antarctica) ice core was analyzed using two electrical methods: AC-ECM and ECM (electrical conductivity measurements). AC-ECM is a method to detect the complex admittance between electrodes dragged on the ice surface with mm-scale resolution and uses 1 V and 1 MHz. The ratio of the real to imaginary part of the admittance is the AC loss factor, which responds linearly to the amount of sulfuric acid and hydrogen ions. Both the AC loss factor and the ECM current respond to acid, but the ECM signal tends to saturate at high acidities. Dome Fuji ice was measured to be highly acidic, with background values of 2–7 μM, and had >500 major peaks with acidities of up to 90 μM. This ice-core evidence and earlier snow-chemistry survey around the dome region indicates that Dome F may have a better connection to the stratosphere than have sites at lower altitude, which allows more stratospheric aerosol and gases to reach the snow surface. Acidity tends to be high in interglacial periods, but correlation between acidity and δ^{18}O is not straightforward. Electrical signals decreased and smoothed out with increasing depth; the diffusion coefficients deduced from this smoothing were $10–10^2$ times greater than in solid ice. The ice core exhibited electromechanical effects and expelling effects from sulfate peaks.

INTRODUCTION

Ice-core records can reveal climate history over time-scales of up to 10^6 years. By resolving ice-core records, we can extract information on past climate, such as temperature, precipitation rates, atmospheric composition, chemical components, and solid material transported to polar regions. In ice-core studies, researchers are often interested in annual or seasonal-scale variations as well as far longer-scale variations such as glacial/interglacial cycles. Detection of such variations from typically km-long samples is time-consuming work that often requires $10^3–10^5$ samples.

Usually, electrical conductivity measurements (ECM) are performed first because such methods are relatively fast and can quickly locate positions of climatic events on the ice cores. The ECM method measures the direct current between two electrodes separated by 10–15 mm with an applied voltage of 350–2000 V (Hammer, 1980; Neftel and others, 1985). These electrodes are moved along a freshly prepared, smooth surface of ice. ECM indirectly measures the acid distribution in ice, although calibration must be done for each measurement system and each ice core. Another method that has been used is dielectric profiling (DEP; Moore and others, 1989; Wolff and others, 1995). Unlike the ECM method, DEP does not drag electrodes along the surface. It measures the high-frequency-limit conductivity and complex permittivity with a spatial resolution of 5–20 mm. The applied voltage is typically 1–3 V. The high-frequency-limit conductivity responds to the amounts of acid, ammonium and chloride in ice cores (Moore and others, 1994; Wolff and others, 1997). Sugiyama and others (1995, 2000) tested a third method, AC-ECM. Sugiyama and others (2000) reported that the conductance at the ice-core surface increases linearly with the concentration of sulfate ions and hydrogen ions. AC-ECM detects high-frequency-limit conduction with an effective spatial resolution of about 10–15 mm, which is the same as ECM. The energy dissipated in the ice by the ECM method was about 10^6 times that from the AC-ECM method because the voltage was 10^3 times greater. Although AC-ECM signals correlate to sulfuric acid and hydrogen ions (Sugiyama and others, 1995, 2000), possible effects from chloride or ammonium found in another AC method, DEP (Moore and others, 1994; Wolff and others, 1997), are still unknown.

From 1992 to 1998, the Japanese Antarctic Research Expedition (JARE) conducted a deep ice-coring project at Dome Fuji (hereafter Dome F), the second highest dome summit in East Antarctica. The location is 77°19′ S, 39°40′ E (3810 m a.s.l.), and the ice thickness is 3028 ± 15 m as measured by radar sounding. The annual mean temperature 10 m below the surface is −58.6°C. The project team recovered ice down to 2503 m, which contains climatic data going back 320 kyr or more (Watanabe and others, 1999).

The purpose of this paper is to report details of the electrical measurements and our analyses of the core. First, we describe the methods, the physical meaning of the signals, and how the treatment of the core affects measurement qual-

https://doi.org/10.3189/172756402781816951 Published online by Cambridge University Press

Table 1. Experimental conditions for AC-ECM and ECM

Core section	Depth	Time lag between core processing and AC-ECM	Temperature range of ice[a] for AC-ECM	for ECM	Average AC loss factor at −25°C	Estimated absolute errors[b]
	m		°C	°C		
I	112.65–229.01	4–5 months	−31 to −38	−23 to −32	0.161	0.015
II	229.01–310.90	3–4 months	−28 to −33	−23 to −32	0.174	0.030[c]
III	310.90–551.46	9 months	−22 to −24	−18 to −26	0.131	0.015
IV	551.46–850.00[d]	None[e]	−23 to −32	Same	0.124	0.015
V	850.00–2251.40	None	−18 to −23	Same	0.104	0.015
VI	2251.40–2503.07	None	−25 to −32	Same	0.055[f]	0.020

[a] Ice temperature was measured using an infrared radiation thermometer.

[b] Error is the standard deviation that appears as systematic error due to errors in calibration for each measurement. This is an absolute error. However, for each individual measurement, errors in variation of signals within a run are about 0.005.

[c] This larger error occurred due to insufficient calibration at the beginning stage of the measurement.

[d] This depth range includes most of the brittle zone which ranges from 500 to 870 m. Ice core was processed at lower temperatures.

[e] AC-ECM and ECM were measured at the same time.

[f] Average loss factor was from depths between 2251.4 and 2380 m.

ity. Second, we present detailed features of the electrical data of the entire ice core. Finally, we present our interpretation in terms of climatic records. We found that the Dome F core is characterized by highly acidic ice presumably from transport of gas and aerosols from the upper troposphere and stratosphere. Also, the combined use of AC-ECM and ECM revealed new implications about electrical conduction in ice, which we discuss in Fujita and others (2002b).

MEASUREMENTS

Methods

After equilibrating for 1 day at the cold-room temperature at Dome F, all core sections, which were 93 mm in diameter and about 1.7 m long, were cut parallel to their central axes into 60% and 40% portions by volume. The cut surfaces of the 60% portions were further finished with a microtome knife to make fresh, smooth surfaces. Further details of the processing are in Fujita and others (2002a). Immediately after a surface was cut and finished, two AC-ECM electrodes were dragged along the surface with a 1 MHz, 1 V signal. Within a few minutes, two ECM electrodes were dragged along the same surface with a 1250 V d.c. potential difference. The entire ice core from depths of 112.65 to 2503.07 m was covered by the measurements using both methods. Although the signal was sampled every 2 mm, we plot only 10 mm running averages of the data to remove noise. The AC-ECM electrodes were manually dragged along the ice at about 1 cm s^{-1}, whereas the ECM electrodes were manually dragged along the ice at about 25 cm s^{-1}.

The AC-ECM system consists of two coaxial electrodes and an auto-balance bridge (HP model 4284A precision LCR meter). It measures the complex admittance $Y^* = G + Bi$, where G is the conductance and B is the susceptance, at the surface of ice using frequencies between 20 Hz and 1 MHz. For further details, see Sugiyama and others (1995, 2000). We primarily used 1 MHz to detect the high-frequency-limit conductance of ice; here high-frequency-limit means frequency well above the Debye dispersion only, and below the dispersions that exist above the microwave region. The electrodes were aligned perpendicular to the core axis and 15 mm apart, and the contact area of each electrode was about 1.0 mm^2. The effective resolution of the electrodes approximately equaled the distance between the electrodes (15 mm); based on a physical principle that the electrical field decreases inversely proportional to the distance from a given location to each electrode, this effective resolution applies both for a.c. and d.c. Within this distance, about 65% of the lines of electrical force cross. The load on the electrodes was of the order of 5×10^5 Pa. Because the AC-ECM needs careful calibration of the auto-balance bridge, cable and electrodes, we calibrated the admittance to measurements on three reference materials: dry air, aluminum and Teflon. We found that insufficient calibration would double the estimated error in the AC loss factor that is shown in Table 1. The AC conductance at −20°C is proportional to the concentration of sulfuric acid and hydrogen ions (Sugiyama and others, 2000). Further details of the AC-ECM measurement method are in Sugiyama and others (1995, 2000).

The ECM system had the same electrode contact areas and separation as the AC-ECM system, although the pressure on the ice was 10 times greater and the applied voltage was 1250 V. The independent laboratory measurements that assess both a.c. and d.c. signals are reported in Fujita and others (2002b).

Measurement history and quality

ECM measurements are known to be affected by the storage age of the ice cores (Hammer, 1983); furthermore, we found that the AC-ECM measurements were affected by the room temperature through the effect of temperature on ice brittleness. Hence, we document the processing conditions here. Ice cores were recovered from July 1995 to December 1996, then the cores were processed and ECM measurements were performed at the coring site from November 1995 to June 1997. AC-ECM was used only from March 1996, that is, 4 months after the processing started; during these 4 months, we had made ECM measurements down to 551.46 m depth. Therefore, all ECM measurements used freshly prepared smooth surfaces, whereas the AC-ECM measurements for depths shallower than 551.46 m could not be performed on the same, freshly prepared surfaces. For these shallow samples, we simply shaved 0.1–0.2 mm of ice off the surface with a microtome knife; hence, the AC-ECM measurements were performed

https://doi.org/10.3189/172756402781816951 Published online by Cambridge University Press

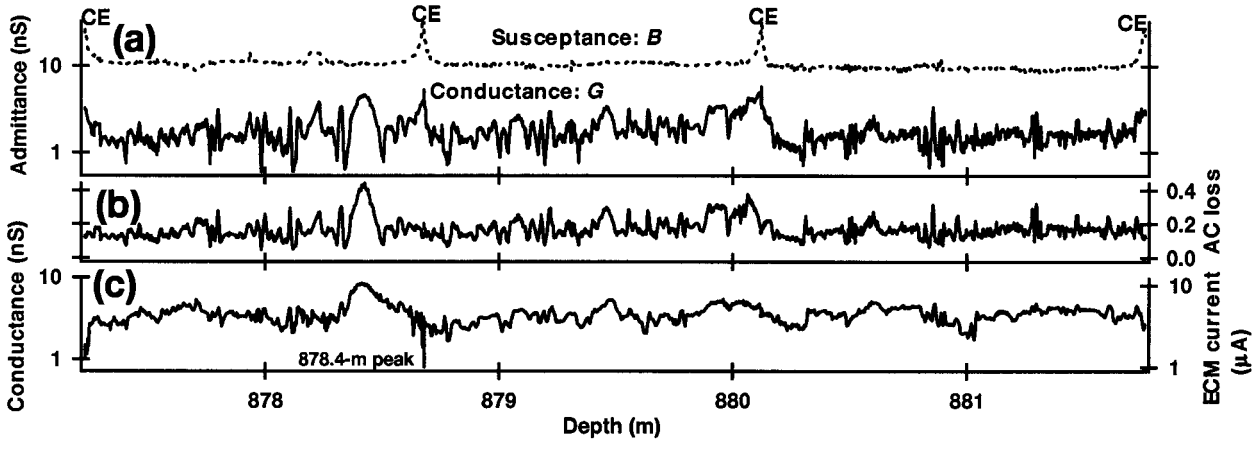

Fig. 1. An example of raw data from the AC-ECM and ECM. (a) Susceptance (dotted lines) and conductance (solid lines) from the AC-ECM. The ordinate uses a logarithmic scale. The graph shows consecutive measurements on three cores, each about 1.5 m long. Core ends are indicated by "CE" because edge effects caused increases of both susceptance and conductance. (b) AC loss factor defined by Equation (1) (linear scale). (c) ECM current (right axis) and d.c. conductance (left axis). The ordinate uses a logarithmic scale. The d.c. conductance is the ratio of ECM current to the applied voltage.

on a surface that was 0.1–0.2 mm within the ice as compared to the surface used for the ECM measurements taken 3–9 months previously (see Table 1). Therefore, we cannot treat equally the a.c. data at depths shallower and at depths deeper than 551.46 m. In addition, we could not strictly control the temperature in the ice-core processing room, for technical reasons. We corrected all the measured data to values at a temperature of −25°C assuming activation energies of 0.25 V for AC-ECM parameters (Sugiyama and others, 2000) and 0.23 V for the ECM current, but possible errors in activation energies could cause systematic errors. Therefore, to determine if core aging or the measurement temperature affected the results, we classify the data into six depth regions (I–VI in Table 1) based on storage age and measurement temperature. In addition, the error estimate of the AC-ECM is affected by its calibration; these error estimates are also shown in Table 1. Most measurements were performed at temperatures between −20° and −30°C. The error estimate in Table 1 does not include possible errors in the activation energies. This error can be larger for measurements at lower temperature; for example, an error by 10% in activation energy for a measurement at −35°C causes about 4% error when corrected to −25°C.

Removing an edge effect

Through a number of measurements at Dome F, we found that both the real (G) and imaginary (B) parts of the complex admittance increased near the core ends, yet their ratio was not significantly affected by this edge effect (Fig. 1). The edge effect is explained by the surface admittance of the core ends. Although the effective resolution was 15 mm, about 35% of the electric field lines exist outside of this resolution. These lines detect the surface admittance at the core ends. The observed features agreed well with the theoretical calculation. To remove the edge effect from the data, we introduce and plot the AC loss factor δ:

$$\delta = \frac{G}{B}\,. \qquad (1)$$

This δ is dimensionless; physically, it measures the energy loss due to electrical conduction in the vicinity of the ice surface during a cycle of the electrical field. Calibration for the AC loss is discussed in Fujita and others (2002b). Figure 1b shows δ calculated from measured values of G and B in region V. The edge effect was removed from the signals in Figure 1a. Apparently, the edge effect only changes coupling of the electrodes to ice: it does not affect the energy loss δ. In contrast, the ECM signal does not show an obvious edge effect (Fig. 1c). ECM current always shows smoother and more nearly uniform features than the AC loss.

RESULTS

The entire record

Figure 2a–d show the entire AC-ECM and ECM records for the 2503 m Dome F ice core. This paper deals with data from ice deeper than 112.59 m. ECM data for ice shallower than 112.59 m are in Watanabe and others (1997).

In Figure 2a, AC loss factor δ ranged from 0 to 2. The AC loss background level is about 0.1, but there are many peak signals ranging from 0.2 to 2. These peak heights decrease with depth and hence with the age of ice. Calibration for the AC loss is discussed in Fujita and others (2002b). Based on linear relations between AC loss, high-frequency-limit conductivity, acidity and the amount of SO_4^{2-} in ice, which were measured on the Dome F core, Fujita and others (2002b) derived a relation between AC loss at −25°C and acidity in μM:

$$[\text{acidity}] = (42 \pm 11)\delta - 1.0 \pm 0.4 \quad (\mu\text{M})\,. \qquad (2)$$

Corroboration is provided later in this paper. The high-frequency-limit conductivity in ice at −21°C is, from Fujita and others (2002b),

$$\sigma = (134.6 \pm 4.8)\delta + 2.7 \pm 1.0 \quad (\mu\text{Sm}^{-1})\,. \qquad (3)$$

These relations between acidity and δ, and between δ and σ, are compatible with the calibrations of DEP (Moore and others, 1994; Wolff and others, 1997). We use Equations (2) and (3) to show the estimated acidity and high-frequency conductivity based on the AC loss factor (Fig. 2a). This acidity scale suggests that many peak signals have an acidity of 20–40 μM. The largest signal was 88 ± 22 μM at 132.30 m depth and the second largest was 52 ± 13 μM at 635.9 m depth, both of which are extremely large acidities compared with previously reported acidity peaks in polar ice sheets. Peak heights seem to decrease significantly with time and depth, which we

https://doi.org/10.3189/172756402781816951 Published online by Cambridge University Press

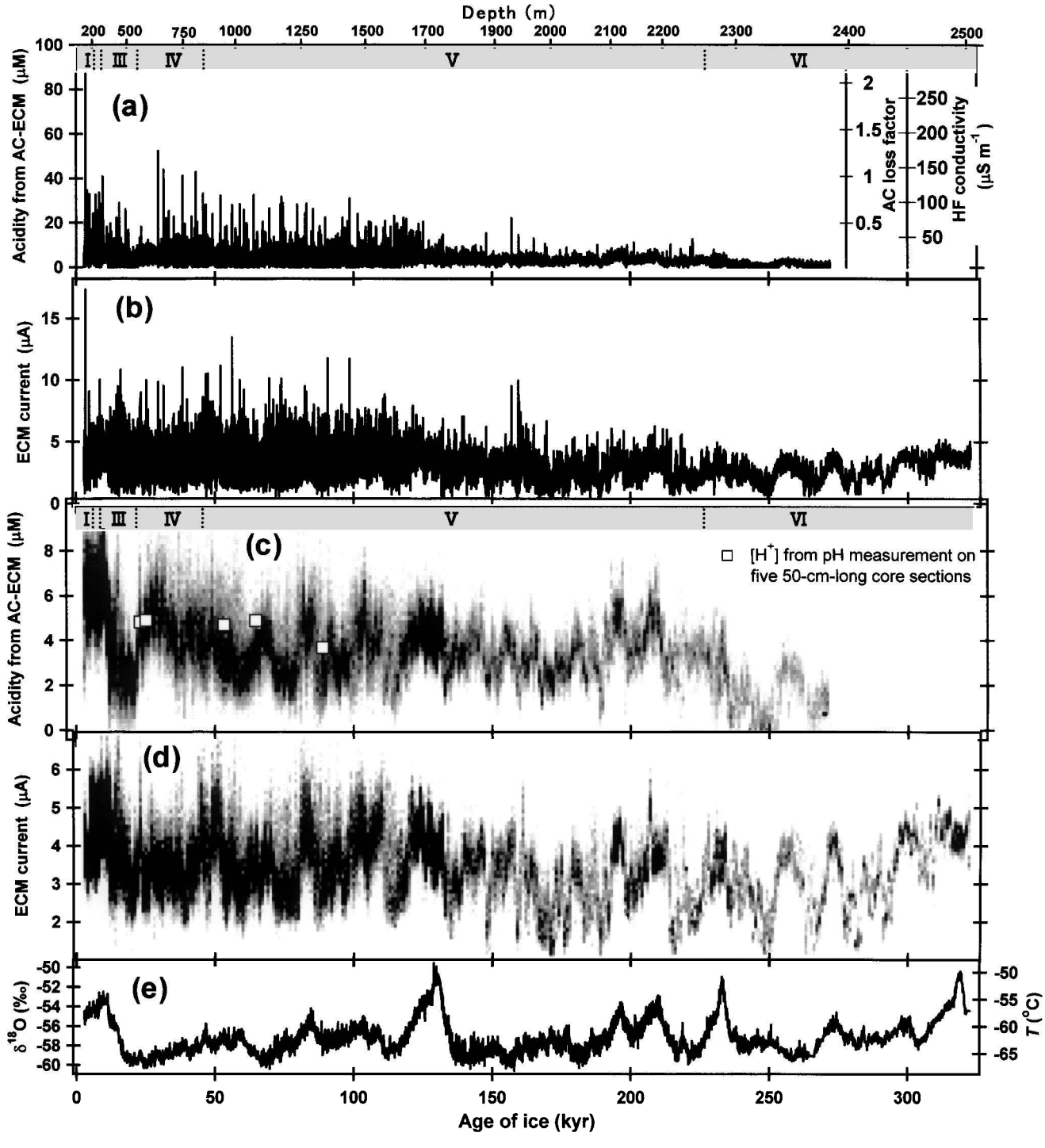

Fig. 2. The entire records of AC-ECM and ECM vs depth of ice (top axis) and, equivalently, age of ice (bottom axis). (a) AC loss factor (one of the right axes) corrected to values of −25°C using an activation energy of 0.25 eV. This was converted to acidity (left axis) using Equation (2), and to high-frequency conductivity (one of right axes) using Equation (3). Symbols I–VI indicate the experimental conditions shown in Table 1. Data from ice deeper than 2390 m were rejected due to a technical problem. (b) ECM current corrected to values of −25°C using an activation energy of 0.23 eV. (c) Acidity calculated from the AC loss factor is the same as in (a), but the density of data within a unit grid size of 10^3 years × 0.2 μM is shown as an arbitrary gray scale. The blackest regions have the most data points for that particular 10^3 year period. This gray-scale image shows the mean tendency of the signal. The open squares are data points from pH measurement of the ice core. Five 50 cm long core segments were used. (d) ECM current as in (b) but plotted as a density plot with unit grid of 10^3 years × 0.1 μA. The density-plot style is the same as in (c). (e) Oxygen isotope profile (Watanabe and others, 1999). The temperature scale in the right axis was calculated from a present-day relation between $\delta^{18}O$ and mean annual surface temperature on the plateau of east Dronning Maud Land (Satow and others, 1999).

assume to be due to a process of diffusion from relatively concentrated regions of charge carriers leading to broader but smaller peaks, particularly below 1700 m. Below about 2250 m, peak signals in the δ data are difficult to identify. We tentatively estimated the diffusion coefficient from the decreases of peak height in Figure 2a. The diffusion length was a few centimeters in the top 1000 m, that is, for 50 kyr. Then the diffusion coefficient is of the order of 10^{-15}–10^{-16} m^2 s^{-1}. This is larger than the self-diffusion coefficient in ice at the same temperature range (215–225 K) (Ramseier, 1967) by one or two orders of magnitude. This suggests that the charge carriers are not migrating via self-diffusion in the ice lattice.

Figure 2b is the entire ECM record corrected to −25°C. The activation energy of 0.23 eV was derived from the entire

https://doi.org/10.3189/172756402781816951 Published online by Cambridge University Press

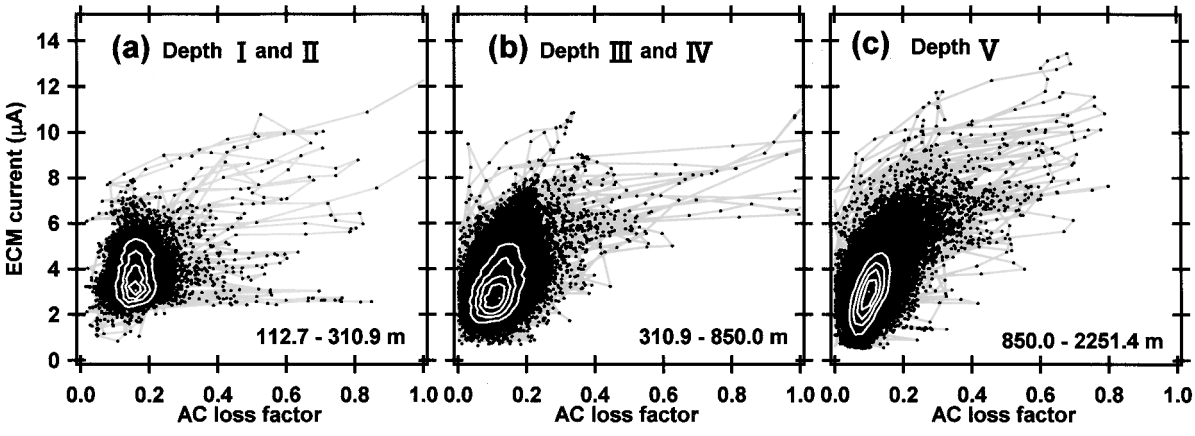

Fig. 3. Plot of ECM current vs AC loss factor at −25°C for three depth levels (Table 1). Consecutive data are connected by gray lines to show depth trajectories of data points (lines connecting data at adjacent depths) at peaks in the AC loss factor. Contour lines are drawn for the densities of 80%, 60%, 40% and 20% of the maximum density.

10 mm averaged ECM data (2.4×10^5 points) of the Dome F ice together with the ice-temperature measurements. We were able to carry out this calculation because of the scatter of temperatures as in Table 1. The fluctuation of the background level is much larger than that from the AC-ECM. Also, peak magnitudes are significantly different from peaks of AC-ECM: large peak signals in δ are often small in the ECM and vice versa. Although the peak signals are always wider than AC-ECM peaks as seen in an example in Figure 1, peak widths increase with increasing depth with amounts comparable to those in the AC-ECM signal. This means that the diffusion coefficients of the charge carriers for the two methods have the same magnitude.

Figure 2c uses the same AC-ECM data as in Figure 2a, but the gray scale shows the probability of existence of a data point at a given time to emphasize the background tendency. Details are given in the figure caption. Figure 2c shows that the interglacial periods tend to correlate with higher levels of acidity. However, the relation between $\delta^{18}O$ and acidity is not straightforward; within the glacial periods there are acidity peaks just as large as those within the interglacial periods. The mean value tends to decrease with depth below about 2200 m. The AC-ECM-based acidity in the background level agreed with the five pH data points in the figure.

Figure 2d uses the same ECM data as in Figure 2b, but the data are plotted as a density plot. The general tendency is similar to that of the acidity in Figure 2c, but at some depth ranges there are significant differences, in particular in region IV. The tendency is clearer in deeper (older) ice because the signals are smoothed due to diffusion. Like the AC loss factor, the mean values tend to decrease with depth and with age of ice (see Fig. 4).

The depth/age calculation was done by H. Shoji and others (personal communication, 2001) using a steady-state flow model developed by Dansgaard and others (1993) for a time-scale calculation of the dome summit ice core. The original model was developed for Greenland, but it was adapted to Dome F. The relation between $\delta^{18}O$ and the annual accumulation rate was derived from the present-day relation observed in east Dronning Maud Land around the dome summit (Satow and others, 1999), and this relation was assumed to hold in the past. Furthermore, a layer containing volcanic dust at 1849.6 m was identified as a volcanic eruption of 141 kyr BP (Fujii and others, 1999) and it was used as a fixed depth/age point.

Relation between AC loss factor and ECM current

Studies of ECM profiles have suggested that the ECM current responds only to the acidity of the ice (Hammer, 1980; Moore and others, 1992; Wolff and others, 1997); however, this method often showed inconsistent responses to the amount of acid in the Dome F ice core (Fujita and others, 2002b). The AC loss factor responds linearly to the amount of sulfuric acid and hydrogen ions (Sugiyama and others, 2000). Chloride or ammonium might have some unknown effects on AC loss, but based on their contribution to the high-frequency-limit conductivity (Moore and others, 1994), their influence on AC loss is likely to be small for the chemical concentrations present at Dome F. Therefore, the inconsistent ECM responses to the amount of acid might explain the large amount of scatter between the entire 10 mm averaged ECM current and the AC loss in Figure 3a–c. At constant ECM current, the AC loss factor can vary from 0 to 1. We define a trajectory as a sequence of data points with increasing depth. The trajectories in Figure 3 suggest that the ECM current increases rapidly along a trajectory when the AC loss is small, but then saturates at larger AC loss factors. These saturation ECM currents tend to be lower in Figure 3a than in Figure 3b and c; in other words, AC loss can increase without apparent increase of the ECM current at shallower depths. Fujita and others (2002b) argue that the scatter in Figure 3 is mainly due to non-linear and variable response of the ECM current to acidity.

Peak widths of AC loss and ECM current

Peak widths of the ECM current i are generally wider and have longer tails trailing towards deeper depths than peak widths of δ. An example is the 878.4 m peak labeled in Figure 1c. Even when the i peak has a long tail towards deeper ice, the corresponding δ peak sometimes decreases rapidly with increasing depth. These sharp decreases are generally clearer on the largest δ peaks and were found only in the δ data. The i always showed different behavior near the peaks compared to the δ. Fujita and others (2002b) describe three examples of δ peaks from the Dome F core that are correlated only to sulfuric acid. Several chemical studies from Greenland ice and Antarctic ice have found that high concentrations of sulfate ions expel other chemical species, presumably as a post-depositional process (e.g. Wagnon and others, 1999). Although finding the cause of the δ drop requires comprehensive chemical analyses, we are interested in the displacement of several

https://doi.org/10.3189/172756402781816951 Published online by Cambridge University Press

Table 2. Multiple regression analysis between AC loss factor and major ions in the core section from 850 to 2250 m

Variable	*Regression coefficient*	*Standard error*	*Partial correlation coefficient*	*VIF*[a]	*Average molarity*
	μM^{-1}				μM
SO_4^{2-}	0.025	0.001	0.48	1.4	1.6
Na^+	−0.020	0.001	−0.37	3.3	2.3
Ca^{2+}	0.015	0.003	0.12	3.1	0.5
Cl^-	0.000	0.000	0.07	1.0	2.7
K^+	0.031	0.016	0.06	1.7	0.1
constant	0.107	0.003			

Notes: Total number of cases used for the analysis is 1257, each of which was typically a 7–10 cm long ice-core segment used for chemical analysis. Multiple-correlation coefficient is 0.57. For the other variables, such as Mg^{2+}, NO_3^-, F^- and NH_4^+, we could not find any statistically significant coefficient to explain variations of the AC loss because the average concentration is small and also because of the possible effect of multicollinearity among several variables. We made no measurement for the H^+ concentration.

[a] Variance inflation factor (VIF) measures multicollinearity; that is, if VIF is large, then there is a high correlation between independent variables.

chemical species expelled by sulfate to explain a number of observed decreases at one or both sides of the peaks.

Electromechanical effect in the brittle zone

Electrical noise, presumably due to crack formation in the core, occurred during the AC-ECM test at depths of 500–870 m, which is mostly in the IV core range. This depth range is characterized as the brittle zone (see Fujita and others, 2002b, fig. 5). The complex admittance was unstable and showed fluctuations in many parts of the ice cores. Electrical noise can be caused by ice cracking (Fifolt and others, 1993).

DISCUSSION

In this section, we assess data quality and calibration for the entire record. For the assessment, we used multiple-regression analysis to see how AC loss correlates with chemical components, in particular, with sulfate. Based on these assessments, we discuss the interpretation of acidity measurements in Dome F ice and its variation in climatic cycles.

Data quality, calibration and aging effect for AC loss factor

Of all the core sections, the 1400 m long section V (Table 1, 850.00–2251.4 m) was measured under the best-controlled conditions. Only this section had all of the following measurement conditions: freshly prepared smooth surfaces for both AC-ECM and ECM; ice temperature remaining within 3°C of −20°C; and a good calibration. In contrast, conditions were not consistent for sections I–IV and VI. For example, in sections I–III, possible aging effect could have decreased the AC loss factor. For section IV, the electromechanical effects and possible error in the activation energy could have affected the results. We examined possible effects from these conditions using multiple-regression analysis on the AC loss data and on the measured major chemical compositions of the Dome F core from Watanabe and others (1999).

For the present data, the AC loss is primarily determined by the sulfuric acid content (Sugiyama and others, 2000; Fujita and others, 2002b). Moore and others (1994) reported that ammonium and chloride increase the high-frequency-limit conductivity in the glacial-period part of Greenland ice cores. For the multiple-regression analysis on section V, the AC loss factor was assumed equal to a summation of linear functions of each chemical constituent. The results are listed in Table 2. The analysis revealed that the most significant effects are from SO_4^{2-} first, with a positive regression coefficient, and second is Na^+, with a negative coefficient. In contrast, Cl^- ions and NH_4^+ ions had insignificant influence on AC loss. A common feature of those ions with little significant effect is that their average molarity was small. This means that the effect was possibly obscured by the dominant effects from SO_4^{2-} and Na^+. However, Cl^- ions are an exception because they have the largest average molarity but a regression coefficient of zero. The variance inflation factors (VIF) in Table 2 show that multicollinearity with other ions cannot explain why Cl^- ions do not have a significant effect on the AC loss factor.

Table 3. Regression coefficients of sulfate to explain AC loss factor for the six examined depth ranges

Core section	*Regression coefficient*	*Standard error*	*Reciprocal of the coefficient*	*Number of cases*
	μM^{-1}	%	μM	
I	0.042	14	24	157
II	0.059	5	17	132
III	0.044	14	23	241
IV	0.041	17	24	121
V	0.025[a]	4	40	1257
VI	0.034	26	29	383

[a] This value is from SO_4^{2-} in Table 2.

The same multiple regression analysis was done for all of the six core sections I–VI. The regression coefficients of SO_4^{2-}, which have greater correlation with AC loss, are listed in Table 3. In section V, the result is from Table 2, and the reciprocal of the regression coefficient for SO_4^{2-} is $40 \pm 2\ \mu M$, which is well within the error of the coefficient in Equation (2). This fact supports the validity of our AC-ECM calibration for section V. The larger regression coefficients for sections I–III suggest that the AC loss at the core surface was more sensitive to sulfate ions in the ice core. We cannot adequately explain this increased sensitivity at the moment. As for section III in Figure 2c, the signal level is lower than signal levels in sections I, II and IV. We deduce that the lower signals might be due to an aging effect that occurred during the 9 month interval when the core was stored, between the ECM measurements and the AC-ECM measurements. Similar aging effects on ECM currents have been reported (Hammer, 1983; Schwander and others, 1983). In future analyses, we will carefully examine the meaning of both the increased sensitivity and the possible aging effect.

Sources of uncertainty in measurements of core section IV are relatively low temperatures and possible effects from the electromechanical properties. The regression coefficient is $(0.041 \pm 0.007) \times 10^6\ M^{-1}$ (Table 3), much larger than in section V. In addition, the mean tendency in section IV in Figure 2c is clearly different from that in Figure 2d. Although we cannot adequately explain either the increased regression coefficient or the difference between Figure 2c and d, multiple-regression analysis showed that sodium and chloride have greater correlation with AC loss than sul-

https://doi.org/10.3189/172756402781816951 Published online by Cambridge University Press

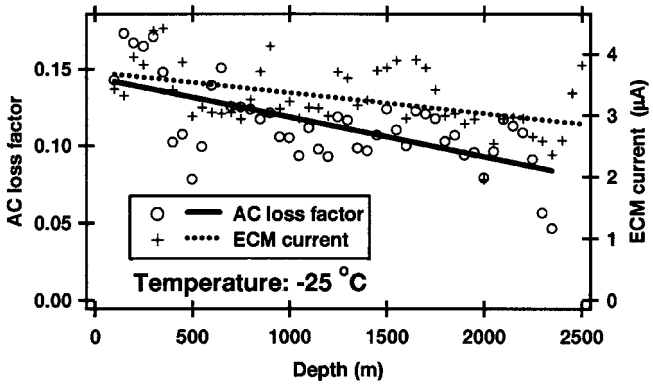

Fig. 4. Decrease of the electrical signals with increasing depths. Data points are averaged values for every 50 m along the core.

fate in sections III and IV. In contrast, sulfate has greater correlation with AC loss in sections I, II and V.

Decrease of signal level with depth

The background values of the AC loss and the ECM current decreased with increasing depth. Although this trend is not clear in Figure 2, Figure 4 shows that the AC loss factor and the ECM current decreased with increasing depth. The decrease of AC loss factor is -0.064 ± 0.011 $(2500\,\mathrm{m})^{-1}$ vs depth and -0.070 ± 0.013 $(300\,\mathrm{kyr})^{-1}$ vs age. Errors are the standard deviation. The decrease of ECM current is -0.84 ± 0.23 $(2500\,\mathrm{m})^{-1}$ vs depth and -0.78 ± 0.23 $(300\,\mathrm{kyr})^{-1}$ vs age. In addition, the average values of AC loss factor in Table 1 demonstrate the depth-related tendency. We cannot identify the major cause by these numbers alone, so this trend should be analyzed along with the electrical conduction mechanism.

Implication of unusually high acidity

Dome F ice has a background acidity derived from δ in the range 2–7 μM. Most peaks are 20–40 μM, but one peak is nearly 90 μM (Fig. 2). The cross-check of the calibration for section V and the several pH measurements for the background acidity (in Fig. 2c) verified that these values are real. These acidities are unusually high compared to other reported values for Antarctic and Greenland ice cores. In the Dome C Antarctic ice core, Holocene ice has a background acidity of 1–1.5 μM and a peak acidity of about 8 μM (Wolff and others, 1999). Many other Antarctic and Greenland ice cores have similar values, although some peaks can be as high as 15–20 μM. The annual accumulation rate at Dome C was 32 mm ice eq. from 1955 to 1978 (Wolff and others, 1999), which is similar to that at Dome F, 28 mm ice eq. from 1995 to 1998 measured using a snow-stake farm. Therefore, the difference in accumulation rates cannot explain the large difference in acidities between Dome F and Dome C. We conclude that the acidity flux is unusually high at Dome F.

Kamiyama and others (1989) discovered that surface snow samples from the inland high plateau in east Dronning Maud Land are characterized by high acidity accompanying the high electrical conductivity, so that the dominant ion is hydrogen, which also couples with chloride and nitrate ions. They reported that the chemical composition differs sharply from that of sea salts. In the inland high plateau, the tritium content increases in the vertical profile of snow pits at depths that correspond to the snow deposition in 1966. This increase is stronger at elevations above 3600 m. All their results suggested that most of the ions contained in snow samples from the inland high plateau, especially higher than 3600 m a.s.l., are not brought directly through the troposphere from the sea around Antarctica but from the upper atmosphere. Furthermore, these ions are affected by physico-chemical reactions occurring in the upper atmosphere. Similarly, the extremely high peak acidities at Dome F are also explainable by the transport of stratospheric aerosols and gases. Large volcanic eruptions can put a lot of sulfate into the stratosphere. Historical eruptions provide sulfate gas and aerosols to both Arctic and Antarctic regions, and thus provide common time-markers in both Antarctic and Greenland ice cores (Langway and others, 1995). Considering the unusually high acidities at Dome F and the spatial distribution in the vicinity as reported by Kamiyama and others (1989), the Dome F region may have a better connection to the stratosphere than have sites at lower altitude, which allows more stratospheric aerosol and gases to reach the snow surface. Generally, researchers have argued that gas and aerosols transport to Antarctica from both hemispheres (e.g. White and Bryson, 1967; Yamazaki and Chiba, 1992), but there seems to be no report that the gas/aerosol transport is particularly concentrated in air sinking on dome summit regions.

These observational facts and interpretations increase the importance of understanding how the Dome F ice core has recorded global-scale environmental changes. Dome F, because it is located at the 3810 m summit, presumably has a better connection to the stratosphere than have sites at lower altitude. Therefore, the core signals reveal climatic records of stratospheric transport. This point should be kept in mind in further interpretations of the Dome F ice-core records.

Climatic changes and acidity

The density plot of acidity derived from the AC loss vs oxygen isotope levels in Figure 5 shows how acidity depends on the atmospheric temperature when the ice first formed. In interglacial periods, acidity tends to be high. But in glacial periods, the relation is not straightforward, as shown in Figure 2a–e. This plot for Dome F contrasts with similar plots for the Greenland ice core (Wolff and others, 1995, figs 17 and 18). In Greenland, ice is acidic in interglacial periods but alkaline in glacial periods; the changes of acid concentration are very large. In contrast, ice is always acidic at Dome F, and typical changes of acidity between glacial and interglacial periods are 2 μM according to the δ measurements and Equation (2). An important difference between Dome F and Greenland is that the former is located in the Southern Hemisphere, which is mostly ocean, whereas the Northern Hemisphere is dominantly covered by continents. The calcareous and other mineral particles tend to neutralize the ice in Greenland. The source for dust in Greenland is supposed to be Asia. The excess dust in Greenland must be due to circumstances at the source and transport paths. Such transport of alkaline dust from possible source areas seems much weaker in Antarctica than in Greenland. Thus, difference in acidity between these locations is basically explained by difference in locations in the global circulation system, but a more complete understanding requires detailed statistical analysis that includes the various chemical constituents and dust components. This should be examined in the future.

https://doi.org/10.3189/172756402781816951 Published online by Cambridge University Press

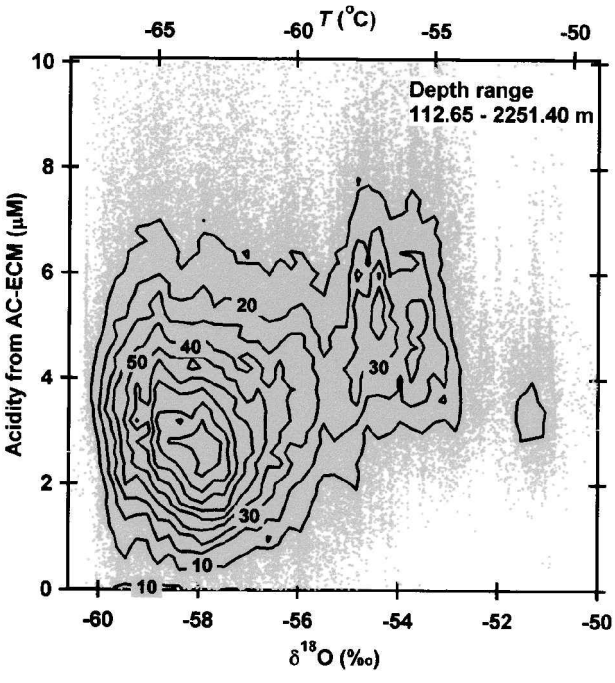

Fig. 5. Plot of acidity derived from the AC loss vs oxygen isotope record. Data points are shown in gray. Contour lines are drawn for every 10% of density, with 100% representing the maximum density in the graph. The tentative temperature scale in the top axis is the same as in Figure 2.

CONCLUDING REMARKS

We have discussed general features of the electrical profiles of the 2503 m ice core including a number of new features. A new measurement method, the AC-ECM, provided significant information for understanding and interpreting the electrical properties of the Dome F ice-core record. The AC-ECM also served to clarify some features of the ECM current that had not been noticed in the latter method's two-decades-long history. However, further examination should be carried out to better understand the electrical conduction mechanism. Although we did not provide insights about specific climatic events or volcanic events, the general information presented here is an important basis for using electrical signals to better understand such events.

We detected extremely high acidity in the Dome F ice. This fact, with the earlier observations by Kamiyama and others (1989), emphasizes the importance of Dome F ice as a record of stratospheric transport of gas and aerosols. The statistical examination and individual examination of the >500 peak signals will be developed elsewhere. The observed electrical phenomena, together with the diffusion process and the electromechanical effects found in the brittle zone, will be examined in the future.

ACKNOWLEDGEMENTS

We thank H. Shoji and others for allowing us to use their ice-core age calibration before their results were published. The data were presented by them in "Dating of the Dome Fuji, Antarctica deep ice core", a presentation at the International Symposium on the Dome Fuji Ice Core and Related Topics, Tokyo, Japan, 27–28 February 2001. This paper is a contribution to the Dome F project conducted by JARE. The authors thank E.W. Wolff and an anonymous reviewer for their critical comments and suggestions.

REFERENCES

Dansgaard, W. *and 10 others*. 1993. Evidence for general instability of past climate from a 250-kyr ice-core record. *Nature*, **364**(6434), 218–220.

Fifolt, D. A., V. F. Petrenko and E. M. Schulson. 1993. Preliminary study of electromagnetic emissions from cracks in ice. *Philos. Mag. B*, **67**(3), 289–299.

Fujii, Y. *and 8 others*. 1999. Tephra layers in the Dome Fuji (Antarctica) deep ice core. *Ann. Glaciol.*, **29**, 126–130.

Fujita, S. *and 8 others*. 2002a. Ice core processing at Dome Fuji station, Antarctica. *Natl. Inst. Polar Res. Mem., Special Issue* 56, 275–286.

Fujita, S. *and 9 others*. 2002b. Linear and non-linear relations between high-frequency-limit conductivity, AC-ECM signals and ECM signals of Dome F Antarctic ice core from a laboratory experiment. *Ann. Glaciol.*, **35** (see paper in this volume).

Hammer, C. U. 1980. Acidity of polar ice cores in relation to absolute dating, past volcanism, and radio-echoes. *J. Glaciol.*, **25**(93), 359–372.

Hammer, C. U. 1983. Initial direct current in the buildup of space charges and the acidity of ice cores. *J. Phys. Chem.*, **87**(21), 4099–4103.

Hondoh, T., *ed.* 2000. *Physics of ice core records*. Sapporo, Hokkaido University Press.

Kamiyama, K., Y. Ageta and Y. Fujii. 1989. Atmospheric and depositional environments traced from unique chemical compositions of snow over an inland high plateau, Antarctica. *J. Geophys. Res.*, **94**(D15), 18,515–18,519.

Langway, C. C., Jr, K. Osada, H. B. Clausen, C. U. Hammer and H. Shoji. 1995. A 10-century comparison of prominent bipolar volcanic events in ice cores. *J. Geophys. Res.*, **100**(D8), 16,241–16,247.

Moore, J. C., R. Mulvaney and J. G. Paren. 1989. Dielectric stratigraphy of ice: a new technique for determining total ionic concentrations in polar ice cores. *Geophys. Res. Lett.*, **16**(10), 1177–1180.

Moore, J. C., E.W. Wolff, H. B. Clausen and C. U. Hammer. 1992. The chemical basis for the electrical stratigraphy of ice. *J. Geophys. Res.*, **97**(B2), 1887–1896.

Moore, J. C., E.W. Wolff, H. B. Clausen, C. U. Hammer, M. R. Legrand and K. Fuhrer. 1994. Electrical response of the Summit–Greenland ice core to ammonium, sulphuric acid, and hydrochloric acid. *Geophys. Res. Lett.*, **21**(7), 565–568.

Neftel, A., M. Andrée, J. Schwander, B. Stauffer and C. U. Hammer. 1985. Measurements of a kind of dc-conductivity on cores from Dye 3. *In* Langway, C. C., Jr, H. Oeschger and W. Dansgaard, *eds. Greenland ice core: geophysics, geochemistry, and the environment*. Washington, DC, American Geophysical Union, 32–38. (Geophysical Monograph 33.)

Ramseier, R. O. 1967. Self-diffusion of tritium in natural and synthetic ice monocrystals. *J. Appl. Phys.*, **38**(6), 2553–2556.

Satow, K., O. Watanabe, H. Shoji and H. Motoyama. 1999. The relationship among accumulation rate, stable isotope ratio and surface temperature on the plateau of east Dronning Maud Land, Antarctica. *Polar Meteorol. Glaciol.*, **13**, 43–52.

Schwander, J., A. Neftel, H. Oeschger and B. Stauffer. 1983. Measurement of direct current conductivity on ice samples for climatological applications. *J. Phys. Chem.*, **87**(21), 4157–4160.

Sugiyama, K., S. Fujita, S. Sueoka, S. Mae and T. Hondoh. 1995. Preliminary measurement of high-frequency electrical conductivity of Antarctic ice with AC-ECM technique. *Proc. NIPR Symp. Polar Meteorol. Glaciol.* 9, 12–22.

Sugiyama, K. *and 7 others*. 2000. Measurement of electrical conductance in ice cores by AC-ECM method. *In* Hondoh, T., *ed. Physics of ice core records*. Sapporo, Hokkaido University Press, 173–184.

Wagnon, P., R. J. Delmas and M. Legrand. 1999. Loss of volatile acid species from upper firn layers at Vostok, Antarctica. *J. Geophys. Res.*, **104**(D3), 3423–3431.

Watanabe, O. *and 12 others*. 1997. Preliminary discussion of physical properties of the Dome Fuji shallow ice core in 1993, Antarctica. *Proc. NIPR Symp. Polar Meteorol. Glaciol.* 11, 1–8.

Watanabe, O., K. Kamiyama, H. Motoyama, Y. Fujii, H. Shoji and K. Satow. 1999. The palaeoclimate record in the ice core from Dome Fuji station, Antarctica. *Ann. Glaciol.*, **29**, 176–178.

White, F. D. J. and R. A. Bryson. 1967. The radiative transfer in the mean meridional circulation of the Antarctic atmosphere during the polar night. *In Polar meteorology*. Geneva, World Meteorological Organization, 199–224. (WMO Tech. Note 87.)

Wolff, E.W., J. C. Moore, H. B. Clausen, C. U. Hammer, J. Kipfstuhl and K. Fuhrer. 1995. Long-term changes in the acid and salt concentrations of the Greenland Ice Core Project ice core from electrical stratigraphy. *J. Geophys. Res.*, **100**(D8), 16,249–16,263.

Wolff, E.W., W. D. Miners, J. C. Moore and J. G. Paren. 1997. Factors controlling the electrical conductivity of ice from the polar regions — a summary. *J. Phys. Chem.*, **101**(32), 6090–6094.

Wolff, E., I. Basile, J.-R. Petit and J. Schwander. 1999. Comparison of Holocene electrical records from Dome C and Vostok, Antarctica. *Ann. Glaciol.*, **29**, 89–93.

Yamazaki, K. and M. Chiba. 1992. Transport simulation of passive tracers from the Northern Hemisphere to the Southern Hemisphere. *Proc. NIPR Symp. Polar Meteorol. Glaciol.* 5, 9–23.